

1 **Preprint of the article**

2 **J.L. Pastor, J.M. Ortega, M. Flor, M.P. López, I. Sánchez, M.A. Climent,**

3 **Microstructure and durability of fly ash cement grouts for micropiles, Construction and**

4 **Building Materials, 117 (2016) 47–57**

5 <http://dx.doi.org/10.1016/j.conbuildmat.2016.04.154>

6 **If you wish a pdf of the published final version of the article, please ask through**

7 **researchgate.net**

8
9
10 **MICROSTRUCTURE AND DURABILITY OF FLY ASH CEMENT**
11 **GROUTS FOR MICROPILES**

12 José L. Pastor, J. Marcos Ortega, María Flor, M. Pilar López, Isidro Sánchez and Miguel A.

13 Climent

14
15 Civil Engineering Department. University of Alicante, P.O. Box 99, 03080, Alicante, Spain.

16 * Corresponding author. isidro.sanchez@ua.es Tel.: +34 965903400 Ext 2090; fax: +34 956903678

17
18 **ABSTRACT**

19 This paper presents a study on the possibility of using fly ash cement as grouts for micropiles.

20 This type of special geotechnical work is commonly used for many applications. Generally,

21 micropiles grouts are prepared using Portland cement, although the standards do not restrict

22 the cement type to use, as long as they achieve a strength requirement. In this research, fly

23 ash cement grouts made with w:c ratios 0.40, 0.45, 0.50 and 0.55 were studied from 2 up to

24 90 days of age. Their microstructure was characterized using the non-destructive impedance

25 spectroscopy technique, electrical resistivity, and mercury intrusion porosimetry. Their

26 durability properties have been studied by determining the water penetration under pressure,
27 and the chloride diffusion coefficient. The compressive strength was also measured and
28 determined, and a maximum water:cement ratio, different for each cement type was obtained.
29 All the results were compared to those obtained for Portland cement grouts. The results
30 obtained confirm that the performance of micropiles made using fly ash cement grouts is
31 adequate, and as it is well known the cements with mineral admixtures provide environmental
32 benefits, so the use of cement including fly ash will contribute to the sustainability, with
33 similar properties to those given by OPC.

34 **Keywords:** micropiles, special geotechnical works, fly ash, durability, microstructure,
35 impedance spectroscopy, water:cement ratio.

36 **1.-INTRODUCTION**

37 In the field of geological engineering, the use of special geotechnical works has become very
38 important. Some of the most commonly used special geotechnical works for civil engineering
39 structures and for building foundations are piles, micropiles, soil anchors and jet grouting
40 injections. There are great differences between those types of works and one of these
41 differences is related to the material in which the steel reinforcement elements are embedded.
42 In the case of the piles, concrete is usually used. However, for micropiles, soil anchors and jet
43 grouting injections, the reinforcement elements are embedded in cement grouts, although
44 mortars might also be used. This fact is very important, because the behaviour of the cement
45 grouts and mortars shows many differences compared to concrete. For example, in general
46 the porosity of hardened grouts is greater than the porosity of concretes [1], [2], and it could
47 influence the durability and mechanical properties of the elements of each particular special
48 geotechnical work. But on the other hand, a higher amount of cement might improve the
49 durability of this type of elements. So, a different performance could be expected if the
50 material used to protect the reinforcement steel elements is cement grout or concrete, as it is

51 usual for the majority of civil engineering structures. Furthermore, the uncertainties can
52 increase as a function of the cement type used, especially if it is used a sustainable cement,
53 which incorporates some kind of active addition, instead of an ordinary Portland cement, as it
54 is the usual practice.

55 Between the different types of grouted special geotechnical works, in the particular case of
56 this research the micropiles have been studied. Micropiles are cylindrical members with
57 diameters of under 300 mm, drilled and grouted with cement grout or mortar injected in one
58 or two phases, reinforced with steel tubing and sometimes strengthened with one or several
59 ribbed bars [3]. In Fig. 1.a and 1.b it is shown an example of micropiles use, and four
60 different sections of a micropile, depending on the type of reinforcement employed [3–5].

61 Regarding the different standards about micropiles materials and implementation existing all
62 over the world, it is important to highlight the Spanish / European Standard for micropile
63 construction UNE-EN 14199 [4] and the US Department of Transportation, Federal Highway
64 Administration's manual entitled Implementation manual for Micropile Design and
65 Construction Guidelines FHWA-SA-97-070 [3]. Moreover, in Spain the Ministry of Internal
66 Development has published a guide for designing and building micropiles in road works [5],
67 which develops and supplements the contents of European micropiles standard [4].

68 Nowadays the global warming constitutes an important environmental problem, and one of
69 the ways to solve it is reducing the CO₂ emission of the industries. In the particular case of
70 cement industry, the use of active additions to improve their sustainability is an important
71 field of study [6–10]. The most popular active additions are ground granulated blast-furnace
72 slag, fly ash and silica fume. In general, these additions are wastes of other industrial

73 processes, but their hydration reaction produces materials similar to those of clinker
74 hydration. So, they can be reused to replace a percentage of this clinker in the cement final
75 manufacture product.

76 As it has been abovementioned, one of the most popular active additions is fly ash, whose
77 effects on the properties of cement-based materials are the object of considerable research [6,
78 11, 12]. One of the main property of this admixture is its capacity for reacting with
79 portlandite, which is a product of the hydration of the calcium silicates of the clinker, through
80 the pozzolanic reactions [11, 13, 14] . New hydrated phases are obtained as products of these
81 reactions that improve the properties of cement-based materials. Fly ash performs very well
82 particularly for structures in marine environments [6, 15–17].

83 Nevertheless, in spite of this good behavior for many uses, the cements containing active
84 additions in general, and especially fly ash, are not commonly used for preparing cement
85 grouts for micropiles. There are not strong reasons which talk out of its use for this purpose.
86 Moreover, regarding other special geotechnical works, the situation is very similar and only
87 there are few studies in this field. One of these researches has been recently published and it
88 deals with the optimization of both the w:c ratio and the binder design, by using silica fume
89 in order to modify the viscosity [18] and to improve the service behavior of cement grouts.
90 With respect to fly ash, there are some studies that claim the feasibility of using fly ash in
91 structural fills, and other geotechnical applications [19, 20]. In view of that, as it has been
92 shown, up to our knowledge the performance of fly ash cements for micropiles grouts has not
93 been studied, especially with regard to their microstructure and durability, despite the fact
94 that there are many evidences that they could produce an improvement compared to ordinary
95 Portland cement. Besides, regarding the compressive strength, fly ash grouts could also
96 perform well, mainly in the long term [21, 22].

97 On this point, in the Spanish / European Standard for micropile construction UNE-EN 14199
98 [4] no cement type is explicitly specified. The only restriction on this aspect is reaching a
99 minimum compressive strength. Similarly, the Ministry of Internal Development's guide for
100 designing and building micropiles in road works [5] and the US Manual FHWA-SA-97-070
101 [3] lay down the minimum compressive strength for micropiles, but not the type of cement to
102 be used and it is acceptable the use of a wide range of water:cement ratios. Despite that, as it
103 has been previously mentioned, at least in Spain cement grouts for micropiles are usually
104 prepared with ordinary Portland cement (CEM I).

105 Then, this research aims to study of the possibility of using fly ash cement as an
106 advantageous material for micropile preparation. To the purpose, the microstructure,
107 durability and mechanical properties of cement grouts for micropiles have been studied. The
108 grouts have been prepared using different dosages (w:c ratios), and using an ordinary
109 Portland cement, and a fly ash-rich commercial cement, to study the viability of using this
110 cement type.

111 The characterization of the microstructure of the grouts has a lot of interest, because it is
112 directly related to the durability properties and the mechanical properties of these materials
113 [23], [24]. In this work, it has also been used non-destructive techniques for studying the
114 grouts porous network, such as impedance spectroscopy [1, 2, 25–27] and electrical
115 resistivity by means of Wenner four-point test [28]. These techniques are nowadays an
116 important research field because they have many advantages, for example the possibility of
117 using the same samples for all the tests throughout the research. This fact permits a better
118 monitoring of the microstructure evolution.

119 In relation to durability of fly ash cement grouts, its study is consequently highly pertinent,
120 especially in the particular context of micropiles, where the reinforcement elements are
121 embedded in the hardened cement grouts instead of concrete, as it has been abovementioned.

122 In this research, water penetration under pressure was the test used to assess durability, due to
123 water is the main vehicle for the ingress of aggressive agents in cement-based materials [23,
124 29]. Grout resistance to chloride ingress was also analysed, inasmuch as these ions are among
125 the primary inducers of steel corrosion, and they can be present in waters and soils in contact
126 with micropiles. The mechanical property studied was compressive strength, since as noted
127 above, this is the main and fundamental parameter specified for codes and standards for
128 determining whether a cement is apt for this application.

129 Finally, because the grouts in these applications harden in contact with the surrounding
130 terrain, exposing it to possible aggressive agents, its properties were characterised from very
131 early ages (2 days) and up to 90 days.

132

133 **2.- EXPERIMENTAL PROCEDURE**

134 **2.1.- Sample preparation**

135 The tests were performed on cement grouts (pastes). These grouts were prepared using two
136 types of commercial cements, a type CEM I 52.5 R/SR Portland cement, (CEM I hereafter),
137 and a pozzolanic cement with a fly ash content from 36 to 55% of total binder, type CEM
138 IV/B(V) 32.5 N (labelled CEM IV hereafter), according to Spanish / European standard
139 UNE-EN 197-1 [30]. The reason for using these commercial cements instead of preparing
140 mixes with ordinary Portland cement and fly ash, is that the accurate preparation of the mixes
141 at the construction site would complicate the process of grouting the micropiles.

142 With regard to the dosage of the grouts, four different water to cement ratios were used: 0.4,
143 0.45, 0.5 and 0.55. As mentioned before, the Spanish guide for designing and building
144 micropiles in road works [5] allows w:c ratios of from 0.4 to 0.55, while Spanish / European
145 standard UNE-EN 14199 [4] specifies that the ratio must be lower than 0.55. Manual FHWA-
146 SA-97-070 [3], in turn, stipulates that the w:c ratio in grout for micropiles must lie between

147 0.4 and 0.5. Then, the w:c ratios studied in this work permit to analyse the influence of this
148 parameter, according to the abovementioned standards. However, it is important to emphasize
149 that in the case of Spain, the grouts are usually prepared with w:c ratio 0.5, in spite of the
150 abovementioned different dosages allowed by the standards and manuals.

151 Several types of specimens were prepared. All the samples were kept in a 95% RH chamber
152 with a temperature of 20°C for 24 hours immediately after setting up the grouts. On one hand,
153 cylindrical specimens were prepared and cast in molds of 10 cm diameter and 15 cm height.
154 After the 24-hours curing time, they were demolded and cut to obtain slices of approximately
155 1 cm thickness. Other cylindrical specimens were cast to diameters of 10 and 15 cm and a
156 height of 30 cm. The 10-cm diameter samples were used to study the variations in electrical
157 resistivity and the 15-cm specimens to determine compressive strength and the penetration of
158 water under pressure. Finally, prismatic specimens with dimensions 4 cm x 4 cm x 16 cm
159 were also prepared (UNE-EN 196-1:2005 [31]) to compare their compressive strength to the
160 strength obtained for the 15-cm diameter x 30-cm high specimens.

161 When the 24-hours curing had finished, all the specimens were submerged in distilled water
162 until the testing age. These curing conditions are intended to simulate the conditions of
163 micropiles that are cast in situ and stay in contact with soil and water from the very first day.
164 The only exception was the 15-cm diameter x 30-cm high specimens, which were stored in a
165 humidity chamber at 20°C and 95% RH as specified in Spanish /European standard UNE-EN
166 12390-2 [32], to which refers the Spanish guide for designing and building micropiles in road
167 works [5] for those particular specimens.

168

169 **2.2.- Mercury intrusion porosimetry**

170 The grouts microstructure was characterized using mercury intrusion porosimetry, as well as
171 the non-destructive techniques previously mentioned. This is a well-known and extensively

172 used technique [33], although it has some drawbacks [34]. The porosimeter employed was an
173 Autopore IV 9500 from Micromeritics. This porosimeter allows determining pore diameters
174 between 5 nm and 0.9 mm. Before the test, samples were oven dried for 48 hours at 50°C.
175 Two measurements were made on each material. Total porosity and pore size distribution
176 were studied through intrusion curves. The tests were performed at 2, 28 and 90 days of age.

177

178 **2.3.- Impedance spectroscopy**

179 The impedance measurements on the cement grouts were carried out using the impedance
180 analyzer Agilent 4294A, which allows capacitance measurements in the range from 10^{-14} F to
181 0.1 F, with a maximum resolution of 10^{-15} F. Impedance spectra of samples were obtained in
182 the frequency range from 100 Hz to 100 MHz, using two different methods. For both
183 methods, the electrodes were circular ($\varnothing = 8$ cm) and made of flexible graphite, attached to a
184 copper piece with the same diameter. First, impedance spectra were obtained with a
185 contacting method, being the electrode in direct contact with the sample. Afterwards, the
186 measurements were also performed using a non-contacting method. This method minimizes
187 the possible contributions of the sample-electrode interface as shown elsewhere [35], and
188 minimizes as well the runaway capacitance existing due to the border effect [36]. It consists
189 of placing a polyester sheet (100 μm thick) between the sample and each electrode. The
190 impedance of the polyester sheets is subtracted from the total impedance measurement, to get
191 only the impedance response of the sample. As this setup gives an almost capacitive
192 impedance spectrum, the answer of the sample is transformed to a spectrum in capacities
193 using the Cole-Cole transformation [1].

194 For validating the obtained impedance spectra, the Kramers–Kronig (K–K) relations were
195 used, to ensure causality, linearity and stability of the measurements [37]. As an example, Fig.
196 2 depicts the Cole-Cole plots at different ages for CEM IV grouts, while Fig. 3 shows the

197 validation of the impedance spectrum of a CEM IV grout using the K-K relations, as
198 mentioned before. The differential impedance analysis was developed by Stoynov et al. [38],
199 and gave excellent results on cementitious materials [1]. It was applied to the spectra before
200 assuming the equivalent circuit as valid for fly ash cement grouts. Fig. 4 shows the result of
201 the analysis on one impedance spectrum. The result is valid for all the data obtained, and the
202 two maxima that shows the plot of the time constant of the material, τ , at each frequency,
203 versus number of points, indicate the presence of two time constants in the impedance
204 spectrum. The number of time constants justifies the fitting of the obtained data to the
205 equivalent circuits proposed by Cabeza et al. [1], which included two time constants. These
206 circuits are shown in Fig. 5. Both circuits have been used for different types of materials [1, 9,
207 27]. The fitting of the measured data to the model proposed is made using a Simplex
208 optimization method, which is described elsewhere [35]. Regarding the impedance
209 parameters, it is important to emphasize that the resistance R_2 and the capacitances C_1 and C_2
210 can be obtained using both contacting and non-contacting methods. In this research, the
211 evolution of those parameters has been studied from non-contacting measurements because
212 of its higher accuracy. For each cement type and w:c ratio four different samples with
213 approximately 1 cm thickness were tested. The evolution of impedance parameters has been
214 followed until 90 days of hardening.

215 The main advantages of using this technique, in addition to being non-destructive, are that the
216 measurement is global, over the whole area of the surface, and it does not give local
217 information on the microstructure of the sample, as the mercury porosimetry does. The non-
218 destructive character allows also to follow the evolution of the microstructure of the same
219 sample over the time, and the rest of available techniques do not allow this follow up. It has
220 to be pointed out here that this technique has been mainly used for OPC samples, where there

221 is not a pozzolanic reaction as it happens in fly ash cements. The possibility of frequent
222 measurement on samples allows to study the effect of this pozzolanic reaction more properly.

223

224 **2.4.- Electrical resistivity**

225 This parameter gives information about connectivity and pore size in a material. In this
226 research the electrical resistivity was determined in cement grouts specimens using the
227 Wenner four-point test described in Spanish standard UNE 83988-2 [39]. This very well-
228 known method is widely used in cement-based materials [40-41]. Specimen electrical
229 resistivity was measured directly on a Proceq analyser.

230

231 **2.5.- Water penetration under pressure**

232 The samples tested were cylinders of 15 cm diameter and 30 cm height according to the
233 Spanish / European standard UNE-EN 12390-8 [42]. The test consists of applying water to
234 the specimens at a pressure of 500 ± 50 kPa for 72 ± 2 hours. When the test had concluded, the
235 samples were split axially and the depth of water penetration was measured in each half.
236 Despite this test is designed for hardened concretes, it was applied here to the cement grout
237 because the standards on micropiles [5] refer to the provisions of Spanish Structural Concrete
238 Code EHE-08 for characterizing most grout properties [43].

239 Regarding the conditioning of the specimens before the test, the standard UNE-EN 12390-8
240 does not specify a certain procedure. Then, in this research the specimens were kept for 72
241 hours prior to the test at a temperature of 20 ± 2 °C and relative humidity of 50%, as suggested
242 the standard. Two samples were tested at 28 and 90 days of age, for each type of cement and
243 w:c ratio. Finally, the results obtained were the mean and maximum depths of the water
244 penetration front for each sample.

245

246 **2.6.- Forced migration test**

247 The study of the resistance against chloride ingress of the hardened cement grouts has a lot of
248 interest. In this research, the forced chloride migration test was performed on water-saturated
249 cement grouts, according to the standard UNE 83987 [44]. The main result obtained is the
250 non-steady-state chloride diffusion coefficient D_{ns} , in m^2/s . Samples of approximately 1 cm
251 thick were tested. The experimental procedure of the test [45] is based on monitoring the
252 anolyte conductivity, which has been shown to be proportional to the chloride concentration
253 of the anolyte.

254 The cement grouts were saturated for 24 hours before the migration tests, according to ASTM
255 Standard C1202-97 [46]. The sample was placed in a cell between two electrolyte containers,
256 whose capacity was 500 ml. The surface of the sample exposed to the migration test was
257 circular of 6.5 cm diameter. The stainless steel electrodes, for establishing the driving electric
258 field, were placed in the apertures of the cell and the distance between them was 25 cm. The
259 catholyte and anolyte chambers were filled with a 1 M NaCl solution and with distilled water,
260 respectively. The applied driving voltage was 12 V, although the effective potential drop
261 between both sides of the cement grout disc was measured periodically. The conductivity
262 measurements of the anolyte solution were performed every 12 hours since the beginning of
263 the test. These measurements were performed with a Crison GLP31 conductimeter, with
264 automatic compensation of the readings to 25°C standard temperature. Temperature data of
265 the electrolytes were also recorded.

266 For each cement type and w:c ratio three different samples were tested. The tests were
267 performed at 2, 28 and 90 days of age. The reason for performing a first test at 2 days has to
268 do with the real service conditions of micropiles. As it has been said before the micropiles
269 stay in contact with soil and water from the moment they are cast. That means that they can
270 be in contact with aggressive substances (in case there are in water or soil) from the very

271 beginning. So, performing that test can give us important information on the real service
272 conditions and the real degradative processes that could take place in a micropile in service,
273 and study the viability of using fly ash cement to construct those elements.

274

275 **2.7.- Determination of compressive strength**

276 As it was stated in the introduction the standards do not restrict the cement type for
277 micropiles, as long as they achieve a compressive strength requirement. The Implementation
278 manual FHWA-SA-97-070 [3] suggests that the neat cement grouts should reach a
279 compressive strength between 28 and 35 MPa at 28 days of age. In the case of standard UNE-
280 EN 14199 [4], the minimum compressive strength required for the grouts at 28 days is 25
281 MPa.

282 The reference standards for micropiles [4, 5] establish that the compressive strength must be
283 determined using cylindrical samples with double length than diameter. For that reason the
284 compressive strength was determined in samples with 15 cm diameter and 30 cm height. The
285 compressive strength was measured following the standard UNE-EN 12390-3:2009 [47].

286 For each condition (cement type and w:c ratio) two measurements were taken.

287

288 **3.- EXPERIMENTAL RESULTS**

289

290 **3.1.- Mercury intrusion porosimetry results**

291 As it was stated in the experimental section two samples were tested for each condition. Fig.
292 6 shows the intrusion curve obtained for CEM I samples tested at 28 days hardening. The
293 results for the two samples are shown, one using continuous line and symbol, and the second
294 measurement made with a dotted line. As it can be seen in Fig. 6 there may be minor
295 differences among the two samples in some cases, but there is a good reproducibility. For the
296 sake of simplicity only one measurement will be shown in the rest of the figures. The second

297 result that could be extracted from this figure is that the increases in w:c ratio increases the
298 total porosity of the samples. This result is general for every cement type and age.
299 A more interesting analysis can be extracted from Fig. 7, where the time evolution of the
300 porosity is studied for samples with w:c ratio 0.5. It can be easily observed that the total
301 porosity decreases with time, but some differences can be seen as a function of the cement
302 type (Fig. 7.a for CEM I results and Fig. 7.b for CEM IV results).
303 First of all, for every studied age the total porosity of the samples prepared with CEM IV is
304 higher than for the samples prepared with CEM I. This result could be also expected since the
305 strength class of CEM IV is lower than the strength class of CEM I (see experimental
306 procedure section). Samples prepared with CEM I show a very small evolution of the pore
307 network between 28 and 90 days, whereas there is a greater evolution for CEM IV samples.
308 This evolution produces a pore network with higher amount of small pore diameter (below
309 100 nm) at 90 days for the CEM IV as compared with CEM I pore network. This evolution
310 and the final pore network are mainly due to the pozzolanic reactions of the fly ash.

311

312 **3.2.- Impedance spectroscopy results**

313 The resistances R_1 and R_2 are related to the pores of the sample which are filled with
314 electrolyte [26]. Changes in the value of the resistance may come from the variation of the
315 pore dimensions, or by the drying of the pores [1, 48, 49]. The evolution with time of
316 resistance R_1 can be observed in Fig. 8 for both types of cement grouts. For CEM I samples,
317 the resistance R_1 kept practically constant or hardly increased with time. At early ages, CEM
318 IV grouts showed lower R_1 values than those observed for CEM I ones. Nevertheless, since
319 approximately 20 days, the resistance R_1 started to increase for CEM IV samples. First, this
320 rise of R_1 was slow and at 30 hardening days the values of this parameter for CEM IV grouts
321 were still lower or similar to those observed for CEM I ones. Since then, the CEM IV R_1

322 values started to increase faster and at 90 hardening days their values were higher compared
323 to CEM I ones.

324 The results of resistance R_2 are depicted in Fig. 9. In general, the evolution of this parameter
325 was very similar to that previously described for resistance R_1 .

326 The changes with hardening time of capacitance C_1 for CEM I and CEM IV specimens are
327 shown in Fig. 10. This capacitance is related to the solid fraction in the samples [26]. For the
328 majority of the samples studied, this parameter increased with time. At early ages, the
329 capacitance C_1 was lower for CEM IV samples than for CEM I ones. At 90 days, this
330 parameter was very similar for both types of cement, or even it was a little higher for CEM
331 IV grouts.

332 The results of capacitance C_2 for both types of cement studied are depicted in Fig. 11. This
333 parameter is related to the pore surface in contact with electrolyte present in the material [48,
334 50]. At early ages, the capacitance C_2 increased with age for CEM I samples and showed
335 higher values than those observed for CEM IV ones. However, it kept practically constant or
336 hardly increased since approximately 20 days for the majority of CEM I grouts. On the other
337 hand, the capacitance C_2 for CEM IV samples showed low values at early ages, but this
338 parameter continuously increased with age, and at 90 days the capacitance C_2 was similar or
339 even higher for CEM IV samples than for those prepared using CEM I.

340

341 **3.3.- Electrical resistivity results**

342 The results of the electrical resistivity measured using the Wenner method are shown in Fig.
343 12. As it can be seen it is noticeable that the values of resistivity for the cement containing fly
344 ash are much higher than for the ordinary Portland cement. Moreover, in the case of cement
345 type IV clearly the higher is the w:c ratio the smaller is the resistivity. The resistivity for both
346 cement types increases with the hardening time.

347

348 **3.4.- Water penetration under pressure**

349 The results of the water penetration under pressure (maximum and average penetration) are
350 shown in Fig. 13. As it can be seen in the plots, the average penetration measured following
351 the standard UNE-EN 12390-8, is always smaller for cement type IV, containing fly ash, than
352 for ordinary Portland cement (CEM I). As could be expected, the increase in the w:c ratio
353 also causes an increase of the average penetration of water in the samples. The values of
354 average penetration show a decreasing tendency with the hardening age for both cement
355 types. The results of the maximum penetration depth are very similar to these about the
356 average penetration depth.

357

358 **3.5.- Forced migration tests**

359 The results of non-steady-state chloride diffusion coefficient (D_{ns}) for CEM I and CEM IV
360 grouts are shown in Fig. 14. This coefficient decreased with age for the majority of CEM I
361 and CEM IV grouts. At all ages, CEM IV grouts showed very low diffusion coefficients in
362 comparison to those observed for CEM I ones.

363

364 **3.6.- Compressive strength results**

365 The results of the compressive strength measured in cylindrical specimens fulfilling the
366 indications of the standard UNE-EN 14199 are shown in Fig. 15. It is clear there that the
367 samples prepared with CEM I have a higher strength than the samples prepared with fly ash
368 cements (CEM IV). This result is in coincidence with the different strength class of the
369 cements used (see section 2.1). The compressive strength increases with time, regardless the
370 cement type and the w:c ratio. As it was explained in the experimental section, the
371 requirement of the standard is that the minimum compressive strength at 28 days should be

372 25 MPa for the grouts. Taking this into account it can be established that both cement types
373 could be used. There is only a limitation in the w:c ratio. For ordinary Portland cement a
374 maximum w:c of 0.5 should be used, while for the fly ash cement a maximum w:c ratio of
375 about 0.45 should be selected.

376

377 **4.- DISCUSSION OF RESULTS**

378

379 The total porosities for CEM IV grouts were higher than those observed for CEM I ones at all
380 hardening ages studied (Fig. 7). This result is consistent with findings reported by other
381 investigations [6, 12, 51]. On the other hand, at early ages (2 and 28 days) CEM IV samples
382 had a coarser porous network than CEM I ones. However, the microstructure of CEM IV
383 grouts was more refined in the long-term, as showed their greater volume of finer pores at 90
384 days (see Fig. 7.b). It is well-known that the portlandite is necessary to start the pozzolanic
385 reactions of fly ash [6, 11, 12, 14] , and it is formed during the clinker hydration. Then, it is
386 needed more time to start the fly ash pozzolanic reactions and, as a consequence, to observe
387 the effects of this addition in the microstructure of the grouts. This fact could explain the pore
388 size distribution of CEM IV grouts in the short-term, especially at 2 hardening days, when it
389 is probably that the degree of development of the pozzolanic reactions of fly ash was very
390 low. Besides, the progressive pore refinement with age showed by CEM IV grouts, could be
391 due to the formation of additional CSH phases [51] as products of fly ash pozzolanic
392 reactions, which leads to a more compact porous structure of fly ash hardened grouts.

393 Regarding impedance spectroscopy results, the resistances R_1 and R_2 are associated with the
394 electrolyte present in the pores of the sample. Since all the samples were kept under
395 immersion, as stated in the experimental section, the changes in the value of the resistances
396 can only come from changes in the pore dimensions [52]. In the short-term, the lower
397 resistances observed for CEM IV grouts (see Fig. 8 and Fig. 9) could be related to the their

398 coarse microstructure, due to the still limited formation of new hydrated products from fly
399 ash pozzolanic reactions, as has been already explained. On the other hand, the important
400 increase with time of the resistances R_1 and R_2 for CEM IV grouts would show a progressive
401 closing of their pore structure, probably related to the development of pozzolanic reactions,
402 as indicated the pore size distribution results. In view of that, the results of resistances R_1 and
403 R_2 corroborate the important pore refinement of grouts microstructure produced by fly ash,
404 previously observed by mercury intrusion porosimetry.

405 The dielectric capacitance C_1 is related to the solid fraction of the samples, then it is expected
406 that this parameter increases as solid formation is produced due to the development of clinker
407 hydration and pozzolanic reactions of fly ash. This parameter is independent of pore size
408 distribution. In general, the capacitance C_1 increased with age for the majority of the samples
409 studied. This would indicate a progressive formation of solid phases. This is in accordance
410 with the abovementioned decrease with age of total porosity. The apparent disagreement
411 among the values of total porosity and capacitance C_1 for samples prepared with different
412 cement types (CEM I and CEM IV) come from the fact of the different chemical composition
413 of the materials, fact that will change the dielectric properties and as a result, the value of the
414 capacitance.

415 The capacitance C_2 is associated with the pore surface in contact with the electrolyte present
416 in the material and it is related to the amount of wet pore surface. Since samples are kept
417 submerged, it is expected that pores would be saturated. So changes in the capacitance C_2
418 would be mainly due to the formation of CSH gel layers on pore walls, which will occupy the
419 pores [26]. These products are deposited on the pore surface and they form rough structures,
420 which increase the specific surface of the pores and the tortuosity of the pore network. This
421 rise of pore specific surface brings about an increase of the solid-electrolyte interface, which
422 entails higher values of capacitance C_2 . In general, the capacitance C_2 increased with age for

423 both types of cement studied. At early ages, the lower values of this parameter were observed
424 for CEM IV grouts. However, in the long-term the capacitance C_2 was similar for CEM I and
425 CEM IV grouts, although it was a little higher for CEM IV ones, see Fig. 11.

426 In general terms, these results are in keeping with pore size distributions obtained using
427 mercury intrusion porosimetry and with the results of resistances R_1 and R_2 . The low
428 capacitances C_2 for CEM IV grouts in the short-term could be due to the scarce development
429 of fly ash pozzolanic reactions, as has been already explained. The important rise with
430 hardening age of this parameter could be related to the formation of additional CSH phases,
431 as products of pozzolanic reactions. These CSH phases would be formed over the existing
432 pore surface, increasing the pore surface, the tortuosity of pore network and the solid-
433 electrolyte interface, as suggest the capacitance C_2 results. Finally, the higher values of this
434 parameter at later ages for CEM IV grouts than those observed for CEM I ones would
435 indicate that their microstructure was more refined, which would corroborate the mercury
436 intrusion porosimetry results.

437 The results of the Wenner resistivity test are coincident with the results of the resistances
438 measured with impedance spectroscopy. This result is the expected, and in agreement with
439 the rest of microstructural characterization. However, the impedance spectroscopy gives a
440 more in deep information, due to the analysis of the capacitances. The resistivity for fly ash
441 cement gives a better correlation of the resistivity with the total porosity.

442 Regarding the results of microstructure characterization, it seems that the use of a fly ash
443 cement for preparing cement grouts for micropiles could produce a more refined porous
444 network of the hardened cement grout (cement paste) in the long-term (90 days), compared to
445 ordinary Portland cement. The microstructure of cement-based materials is related to their
446 service properties and especially to their durability [24]. As a consequence it could be
447 expected an improvement of the micropiles durability if they are made using a fly ash cement.

448 Besides, the use of this type of cement would also bring about an increasing of the initiation
449 period of steel corrosion, which would extend the expected service life of the micropiles.

450 With regard to w:c ratio, the results obtained indicate that this parameter does not seem to
451 produce so much influence on the microstructure of cement grouts as the type of cement,
452 except the expected increase of porosity when the w:c ratio is higher.

453 Finally, it is worth to emphasize that the results of the non-destructive technique of
454 impedance spectroscopy are in agreement with those obtained using mercury intrusion
455 porosimetry.

456 The results of water penetration under pressure show that there is a bigger influence of the
457 smaller pore dimensions than of the total porosity. That is the reason why the penetration of
458 water under pressure is lower for cement containing fly ash than for ordinary Portland cement.

459 This result is essential for the use of CEM type IV to grout micropiles. The penetration of
460 water is one of the main durability indicators [23], and this result confirms that the aggressive
461 will have a smaller penetration in the micropiles made of CEM IV, and so will the aggressive
462 substances, so these cement types, in addition to being more sustainable, will guarantee in a
463 more efficient way the durability of the micropiles.

464 Chlorides can produce the corrosion of reinforcing steel bars and pipes, especially in
465 micropiles in contact with waters with high contents of this aggressive. The non-steady-state
466 chloride diffusion coefficient showed much lower values for CEM IV grouts at all ages than
467 for CEM I ones, as it can be seen in Fig. 14. Many studies have demonstrated that the use of
468 fly ash produces a substantial improvement in chloride ingress resistance [53, 54] . The low
469 diffusion coefficients of CEM IV grouts in the short-term, even though the cement paste is
470 more porous, and with bigger pores, can be explained as being a consequence of the higher
471 binding capacity of fly ash cement, as compared to Portland cement. This binding capacity is
472 due to the high content of calcium aluminates brought by the ash [53]. At later ages, the

473 higher microstructure refinement could also contribute to the decrease of chloride diffusion
474 coefficient observed for CEM IV grouts, besides the abovementioned binding capacity of fly
475 ash.

476 The results of the chloride diffusion coefficient would confirm the fact that the use of fly ash
477 cement for preparing cement grouts for micropiles would produce an improvement of their
478 durability, not forgetting the economic and environmental benefits that bring the use of a
479 waste such as the fly ash. Moreover, it is important to emphasize that at 90 hardening days,
480 the non-steady-state chloride diffusion coefficient for CEM IV grouts were very similar for
481 samples prepared with w:c ratios between 0.4 and 0.55.

482 The results of the compressive strength, as it was explained in the results section limit the
483 maximum w:c ratio, that is not in compliance with the standard, so, from the point of view of
484 the application of these cements for micropiles grouting this parameter should be controlled
485 before using them.

486 In order to check the possibility of injecting the grouts to prepare micropiles, its fluidity was
487 measured. The results of the fluidity of all the tested cement grouts, are shown in Table 1. As
488 it can be seen in the table the fly ash cement shows a greater workability than the ordinary
489 Portland cement, as it is reported in the literature [55-59]. As it can be seen in the table the
490 lower is the w:c ratio the better is the fluidity of the fly ash cement compared with the
491 ordinary Portland cement. This result proves that even though the fly ash cement requires a
492 lower w:c ratio to achieve the minimum resistance, it could be pumped to prepare the
493 micropiles in the same conditions as the CEM I.

494

495 **5.- CONCLUSIONS**

496 The main conclusions that can be drawn from the results previously discussed can be
497 summarized as follows:

- 498 1. The cement grouts made using fly ash cement exhibited higher microstructure
499 refinement in the long-term (90 hardening days) than those prepared using ordinary
500 Portland cement.
- 501 2. The use of fly ash cement for micropiles grouts produced an important improvement
502 of their resistance against chloride ingress.
- 503 3. The results of the non-destructive technique of impedance spectroscopy were in
504 keeping with those obtained using mercury intrusion porosimetry. In view of that, the
505 impedance spectroscopy can be used for studying the microstructure development of
506 fly ash cement grouts. The resistivity gives only results about resistance, which are
507 consistent with the results of impedance spectroscopy.
- 508 4. The penetration of water under pressure guarantees the lower penetration of water
509 and/or aggressive substances in the micropiles prepared with fly ash cement, giving a
510 more sustainable and durable structure.
- 511 5. The reduced porosity of the cement matrix due to the lowering of the w:c ratio has
512 certainly a positive effect on the durability in general. In the case of the resistance to
513 chloride penetration, the effect of w:c ratio on this resistance is less evident as this
514 parameter is influenced by the ability of the matrix to bind chlorides. However, the
515 w:c ratio is determinant from the point of view of the compressive strength, and has to
516 be taken into account to fulfill the minimum values required by the standards.
- 517 6. In view of the results obtained in this research, and under these conditions, the
518 performance of micropiles made using fly ash cement grouts is adequate compared to
519 ordinary Portland cement grouts.

520

521 **6.- ACKNOWLEDGMENTS**

522 This work has been financially supported by the “Ministerio de Economía y Competitividad”
523 (formerly “Ministerio de Ciencia e Innovación”) of Spain and FEDER through projects
524 BIA2010-20548 and BIA2011-25721, and the University of Alicante through project
525 GRE13-25. M. Pilar López is indebted to the government of Spain for a fellowship of the
526 “Formación de Personal Investigador (FPI)” programme (reference BES-2011-046401).
527 Authors would like to thank Cemex España, S.A. and Cementos Portland Valderrivas, S.A.
528 for providing the cements studied in this work.

529

530 7.- REFERENCES

- 531 [1] M. Cabeza, P. Merino, A. Miranda, X. R. Nóvoa, and I. Sanchez, “Impedance
532 spectroscopy study of hardened Portland cement paste,” *Cem. Concr. Res.*, vol. 32, no.
533 6, pp. 881–891, Jun. 2002.
- 534 [2] I. Sánchez, X. R. Nóvoa, G. de Vera, and M. A. Climent, “Microstructural
535 modifications in Portland cement concrete due to forced ionic migration tests. Study
536 by impedance spectroscopy,” *Cem. Concr. Res.*, vol. 38, no. 7, pp. 1015–1025, Jul.
537 2008.
- 538 [3] S. Armour, T.; Groneck, P.; Keeley, J.; and Sharma, “Micropile Design and
539 Construction Guidelines – Implementation Manual Report FHWA-SA-97-070,” *Fed.*
540 *Highw. Adm. – US Dep. Transp. Vancouver*, p. 376, 2000.
- 541 [4] AENOR, “UNE-EN 14199: Ejecución de Trabajos Geotécnicos Especiales:
542 Micropilotes.” p. 54 pp, 2006.
- 543 [5] S. Dirección General de Carreteras, Ministerio de Fomento, Madrid, “Instrucciones de
544 Construcción, “Guía para el Proyecto y la Ejecución de Micropilotes en Obras de
545 Carretera.” Madrid, p. 142, 2005.
- 546 [6] J. Bijen, “Benefits of slag and fly ash,” *Constr. Build. Mater.*, vol. 10, no. 5, pp. 309–
547 314, Jul. 1996.
- 548 [7] R. Demirboğa, “Thermal conductivity and compressive strength of concrete
549 incorporation with mineral admixtures,” *Build. Environ.*, vol. 42, no. 7, pp. 2467–2471,
550 Jul. 2007.
- 551 [8] E. Ganjian and H. S. Pouya, “The effect of Persian Gulf tidal zone exposure on
552 durability of mixes containing silica fume and blast furnace slag,” *Constr. Build.*
553 *Mater.*, vol. 23, no. 2, pp. 644–652, Feb. 2009.
- 554 [9] J. M. Ortega, I. Sánchez, and M. A. Climent, “Influencia de diferentes condiciones de
555 curado en la estructura porosa y en las propiedades a edades tempranas de morteros
556 que contienen ceniza volante y escoria de alto horno,” *Mater. Construcción*, vol. 63,
557 no. 310, pp. 219–234, Mar. 2012.
- 558 [10] T. Ponikiewski and J. Gołaszewski, “The effect of high-calcium fly ash on selected

- 559 properties of self-compacting concrete,” *Arch. Civ. Mech. Eng.*, vol. 14, no. 3, pp.
560 455–465, May 2014.
- 561 [11] V. G. Papadakis, “Effect of fly ash on Portland cement systems,” *Cem. Concr. Res.*,
562 vol. 29, no. 11, pp. 1727–1736, Nov. 1999.
- 563 [12] A. Wang, C. Zhang, and W. Sun, “Fly ash effects,” *Cem. Concr. Res.*, vol. 34, no. 11,
564 pp. 2057–2060, Nov. 2004.
- 565 [13] P. Chindapasirt, S. Homwuttiwong, and V. Sirivivatnanon, “Influence of fly ash
566 fineness on strength, drying shrinkage and sulfate resistance of blended cement
567 mortar,” *Cem. Concr. Res.*, vol. 34, no. 7, pp. 1087–1092, Jul. 2004.
- 568 [14] T. Nochaiya, W. Wongkeo, and A. Chaipanich, “Utilization of fly ash with silica fume
569 and properties of Portland cement–fly ash–silica fume concrete,” *Fuel*, vol. 89, no. 3,
570 pp. 768–774, Mar. 2010.
- 571 [15] M. D. A. Thomas and J. Matthews, “Performance of pfa concrete in a marine
572 environment—10-year results,” *Cem. Concr. Compos.*, vol. 26, no. 1, pp. 5–20, Jan.
573 2004.
- 574 [16] W. Chalee, C. Jaturapitakkul, and P. Chindapasirt, “Predicting the chloride
575 penetration of fly ash concrete in seawater,” *Mar. Struct.*, vol. 22, no. 3, pp. 341–353,
576 Jul. 2009.
- 577 [17] W. Chalee, P. Ausapanit, and C. Jaturapitakkul, “Utilization of fly ash concrete in
578 marine environment for long term design life analysis,” *Mater. Des.*, vol. 31, no. 3, pp.
579 1242–1249, Mar. 2010.
- 580 [18] M. Sonebi, “Optimization of Cement Grouts Containing Silica Fume and Viscosity
581 Modifying Admixture,” *J. Mater. Civ. Eng.*, vol. 22, no. 4, pp. 332–342, Apr. 2010.
- 582 [19] A. Pekrioglu, A. G. Doven, and M. T. Tumay, “Fly ash utilization in grouting
583 applications,” in *Geotechnical Special Publication*, 2003, no. 120 II, pp. 1169–1179.
- 584 [20] A. G. Doven and A. Pekrioglu, “Material Properties of High Volume Fly Ash Cement
585 Paste Structural Fill,” *J. Mater. Civ. Eng.*, vol. 17, no. 6, pp. 686–693, Dec. 2005.
- 586 [21] R. Siddique, “Properties of self-compacting concrete containing class F fly ash,” *Mater.*
587 *Des.*, vol. 32, no. 3, pp. 1501–1507, Mar. 2011.
- 588 [22] F. Faleschini, M. A. Zanini, K. Brunelli, and C. Pellegrino, “Valorization of co-
589 combustion fly ash in concrete production,” *Mater. Des.*, vol. 85, pp. 687–694, Nov.
590 2015.
- 591 [23] V. Baroghel-Bouny, “Water vapour sorption experiments on hardened cementitious
592 materials,” *Cem. Concr. Res.*, vol. 37, no. 3, pp. 414–437, Mar. 2007.
- 593 [24] I. Sánchez, M. P. López, and M. A. Climent, “Effect of Fly Ash on Chloride Transport
594 through Concrete: Study by Impedance Spectroscopy.,” in *12th International Congress*
595 *on the Chemistry of Cement.*, 2007, p. Durability and Degradation of Cement Systems:
596 Corr.
- 597 [25] W. J. McCarter and R. Brousseau, “The A.C. response of hardened cement paste,”
598 *Cem. Concr. Res.*, vol. 20, no. 6, pp. 891–900, Nov. 1990.
- 599 [26] M. Cabeza, M. Keddou, X. R. Nóvoa, I. Sánchez, and H. Takenouti, “Impedance
600 spectroscopy to characterize the pore structure during the hardening process of

- 601 Portland cement paste,” *Electrochim. Acta*, vol. 51, no. 8–9, pp. 1831–1841, Jan. 2006.
- 602 [27] I. Sánchez, M. P. López, J. M. Ortega, and M. Á. Climent, “Impedance spectroscopy:
603 An efficient tool to determine the non-steady-state chloride diffusion coefficient in
604 building materials,” *Mater. Corros.*, vol. 62, no. 2, pp. 139–145, Feb. 2011.
- 605 [28] U. M. Angst and B. Elsener, “On Applicability of Wenner Method for Resistivity
606 Measurements of Concrete,” *ACI Mater. J.*, vol. 111, no. 6, pp. 661–672, Dec. 2014.
- 607 [29] C.-L. Lee, R. Huang, W.-T. Lin, and T.-L. Weng, “Establishment of the durability
608 indices for cement-based composite containing supplementary cementitious materials,”
609 *Mater. Des.*, vol. 37, pp. 28–39, May 2012.
- 610 [30] AENOR, “UNE-EN 197-1:2011. Composición, especificaciones y criterios de
611 conformidad de los cementos comunes.” p. 30, 2000.
- 612 [31] AENOR, “UNE-EN 196-1:2005. Métodos de ensayo de cementos. Parte 1:
613 Determinación de resistencias mecánicas.” 2005.
- 614 [32] AENOR, “UNE-EN 12390-2:2009. Ensayos de hormigón endurecido. Parte 2:
615 Fabricación y curado de probetas para ensayos de resistencia.” 2009.
- 616 [33] S. Diamond, “Aspects of concrete porosity revisited,” *Cem. Concr. Res.*, vol. 29, no. 8,
617 pp. 1181–1188, Aug. 1999.
- 618 [34] S. Diamond, “Mercury porosimetry,” *Cem. Concr. Res.*, vol. 30, no. 10, pp. 1517–
619 1525, Oct. 2000.
- 620 [35] M. Keddad, H. Takenouti, X. R. Nóvoa, C. Andrade, and C. Alonso, “Impedance
621 measurements on cement paste,” *Cem. Concr. Res.*, vol. 27, no. 8, pp. 1191–1201, Aug.
622 1997.
- 623 [36] I. Sánchez, C. Antón, G. de Vera, J. M. Ortega, and M. A. Climent, “Moisture
624 Distribution in Partially Saturated Concrete Studied by Impedance Spectroscopy,” *J.*
625 *Nondestruct. Eval.*, vol. 32, no. 4, pp. 362–371, Jul. 2013.
- 626 [37] E. Barsoukov and J. R. Macdonald, *Impedance Spectroscopy*. Hoboken, NJ, USA:
627 John Wiley & Sons, Inc., 2005.
- 628 [38] Z. Vladikova, D; Zoltowski, P., Makowska, E., Stoynev, “Selectivity study of the
629 differential impedance analysis—comparison with the complex non-linear least-
630 squares method,” *Electrochim. Acta*, vol. 47, no. 18, pp. 2943–2951, Jul. 2002.
- 631 [39] AENOR, “UNE 83988-2:2014, Durabilidad del hormigón. Métodos de ensayo.
632 Determinación de la resistividad eléctrica. Parte 2: Método de las cuatro puntas o de
633 Wenner.” 2014.
- 634 [40] R. Polder, C. Andrade, B. Elsener, Ø. Vennesland, J. Gulikers, R. Weidert, and M.
635 Raupach, “Test methods for on site measurement of resistivity of concrete,” *Mater.*
636 *Struct.*, vol. 33, no. 10, pp. 603–611, Dec. 2000.
- 637 [41] A. Lübeck, A. L. G. Gastaldini, D. S. Barin, and H. C. Siqueira, “Compressive strength
638 and electrical properties of concrete with white Portland cement and blast-furnace
639 slag,” *Cem. Concr. Compos.*, vol. 34, no. 3, pp. 392–399, Mar. 2012.
- 640 [42] AENOR, “UNE-EN 12390-8:2009. Ensayos de hormigón endurecido. Parte 8:
641 Profundidad de penetración de agua bajo presión.” 2009.

- 642 [43] Comisión permanente del, “Instrucción de hormigón estructural EHE-08.” Ministerio
643 de Fomento, Madrid, 2008.
- 644 [44] AENOR, “UNE 83987:2014. Durabilidad del hormigón. Métodos de ensayo.
645 Determinación de los coeficientes de difusión de los iones cloruro en el hormigón
646 endurecido. Método multirrégimen.” p. 9, 2009.
- 647 [45] M. Castellote, C. Andrade, and C. Alonso, “Measurement of the steady and non-
648 steady-state chloride diffusion coefficients in a migration test by means of monitoring
649 the conductivity in the anolyte chamber. Comparison with natural diffusion tests,”
650 Cem. Concr. Res., vol. 31, no. 10, pp. 1411–1420, Oct. 2001.
- 651 [46] ASTM, “ASTM C1202 - 12 Standard Test Method for Electrical Indication of
652 Concretes Ability to Resist Chloride Ion Penetration.” ASTM. Book of Standards
653 Volume: 04.02, 2012.
- 654 [47] AENOR, “UNE-EN 12390-3:2009. Ensayos de hormigón endurecido. Parte 3:
655 Determinación de la resistencia a compresión de probetas.” 2009.
- 656 [48] M. C. Alonso, I. Sánchez, M. Sánchez, M.A. Climent, “Impedance spectroscopy to
657 characterise microstructural changes in liquid and solid phases of mortars exposed to
658 high temperature,” in *2nd International RILEM Workshop on Concrete Spalling due to*
659 *Fire Exposure*, 2011, pp. 43 – 51.
- 660 [49] J. M. Ortega, I. Sánchez, and M. A. Climent, “Impedance spectroscopy study of the
661 effect of environmental conditions in the microstructure development of OPC and slag
662 cement mortars,” *Arch. Civ. Mech. Eng.*, vol. 15, no. 2, pp. 569–583, Feb. 2015.
- 663 [50] P. Chindaprasirt, C. Jaturapitakkul, and T. Sinsiri, “Effect of fly ash fineness on
664 compressive strength and pore size of blended cement paste,” *Cem. Concr. Compos.*,
665 vol. 27, no. 4, pp. 425–428, Apr. 2005.
- 666 [51] P. Wedding, D. Manmohan, and P. Mehta, “Influence of Pozzolanic, Slag, and
667 Chemical Admixtures on Pore Size Distribution and Permeability of Hardened Cement
668 Pastes,” *Cem. Concr. Aggregates*, vol. 3, no. 1, p. 63, Jul. 1981.
- 669 [52] J. M. Ortega, “Microestructura y durabilidad de morteros con cementos que contienen
670 escorias de alto horno y cenizas volantes,” PhD thesis (only available in Spanish),
671 Universidad de Alicante, Alicante, 2011.
- 672 [53] F. Leng, N. Feng, and X. Lu, “An experimental study on the properties of resistance to
673 diffusion of chloride ions of fly ash and blast furnace slag concrete,” *Cem. Concr. Res.*,
674 vol. 30, no. 6, pp. 989–992, Jun. 2000.
- 675 [54] K. O. Ampadu, K. Torii, and M. Kawamura, “Beneficial effect of fly ash on chloride
676 diffusivity of hardened cement paste,” *Cem. Concr. Res.*, vol. 29, no. 4, pp. 585–590,
677 Apr. 1999.
- 678 [55] A. Bras, F. M. A. Henriques, and M. T. Cidade, “Effect of environmental temperature
679 and fly ash addition in hydraulic lime grout behaviour,” *Constr. Build. Mater.*, vol. 24,
680 no. 8, pp. 1511–1517, Aug. 2010.
- 681 [56] K. Turk, “Viscosity and hardened properties of self-compacting mortars with binary
682 and ternary cementitious blends of fly ash and silica fume,” *Constr. Build. Mater.*, vol.
683 37, pp. 326–334, Dec. 2012.
- 684 [57] M. Coö and T. Pheeraphan, “Effect of sand, fly ash, and coarse aggregate gradation on

- 685 preplaced aggregate concrete studied through factorial design,” *Constr. Build. Mater.*,
686 vol. 93, pp. 812–821, Sep. 2015.
- 687 [58] L. Chandra and D. Hardjito, “The Impact of Using Fly Ash, Silica Fume and Calcium
688 Carbonate on the Workability and Compressive Strength of Mortar,” *Procedia Eng.*,
689 vol. 125, pp. 773–779, 2015.
- 690 [59] Y.-W. Choi, M.-S. Park, B.-K. Choi, and S.-R. Oh, “A Study on the Evaluation of
691 Field Application of High-Fluidity Concrete Containing High Volume Fly Ash,” *Adv.*
692 *Mater. Sci. Eng.*, vol. 2015, pp. 1–7, 2015.
- 693

LIST OF FIGURES:

Fig. 1 – (a) Schematic representation of a road tunnel cross-section whose crown is supported by an umbrella of micropiles reinforced with steel pipe (left) and different sections of a micropile, depending on the type of reinforcement employed (right). (b) Excavation process of a tunnel face stabilized using a subhorizontal micropiles umbrella [3-5].

Fig. 2 – Evolution of the Cole–Cole plots for a CEM IV grout prepared with w:c ratio 0.4, obtained using the non-contacting method.

Fig. 3 – Example of an impedance spectrum obtained for a CEM IV grout with w:c ratio 0.5 at 54 hardening days, validated using the Kramers–Kronig (K–K) relations, see the text for details.

Fig. 4 – Differential impedance analysis of the impedance spectrum shown in Fig. 3. The

presence of two maxima in the plot reveals the presence of two time constants in the impedance spectrum.

Fig. 5 – Equivalent circuits with two time constants proposed by Cabeza et al.[1] and used for the fitting of the impedance spectra obtained for samples using the contacting method (a) and the non-contacting method (b).

Fig.6 – Variation of the intrusion curves with w:c ratio for CEM I samples after 28 days hardening. Two samples were tested for each condition and the duplicate results are also shown in the graph

Fig.7 – Curves of intrusion volume for CEM I and CEM IV grouts with w:c ratio 0.5 for all the tested ages

Fig.8– Results of resistance R_1 for CEM I and CEM IV grouts.

Fig.9 – Results of resistance R_2 for CEM I and CEM IV grouts.

Fig.10 – Results of capacitance C_1 for CEM I and CEM IV grouts.

Fig.11 – Results of capacitance C_2 for CEM I and CEM IV grouts.

Fig.12 - Results of electrical resistivity as a function of cement type, w:c ratio and age

Fig.13 - Results of water penetration under pressure as a function of cement type, w:c ratio and age. The average penetration is depicted using a continuous line, while the maximum penetration is depicted with a dotted line.

Fig.14 – Results of non-steady-state chloride diffusion coefficient (D_{ns}) for CEM I and CEM IV grouts.

Fig.15 - Results of compressive strength for CEM I and CEM IV grouts as a function of w:c ratio and age. Red line at 25 MPa denotes the minimum required strength at 28 days by the Spanish standard.

FIGURES

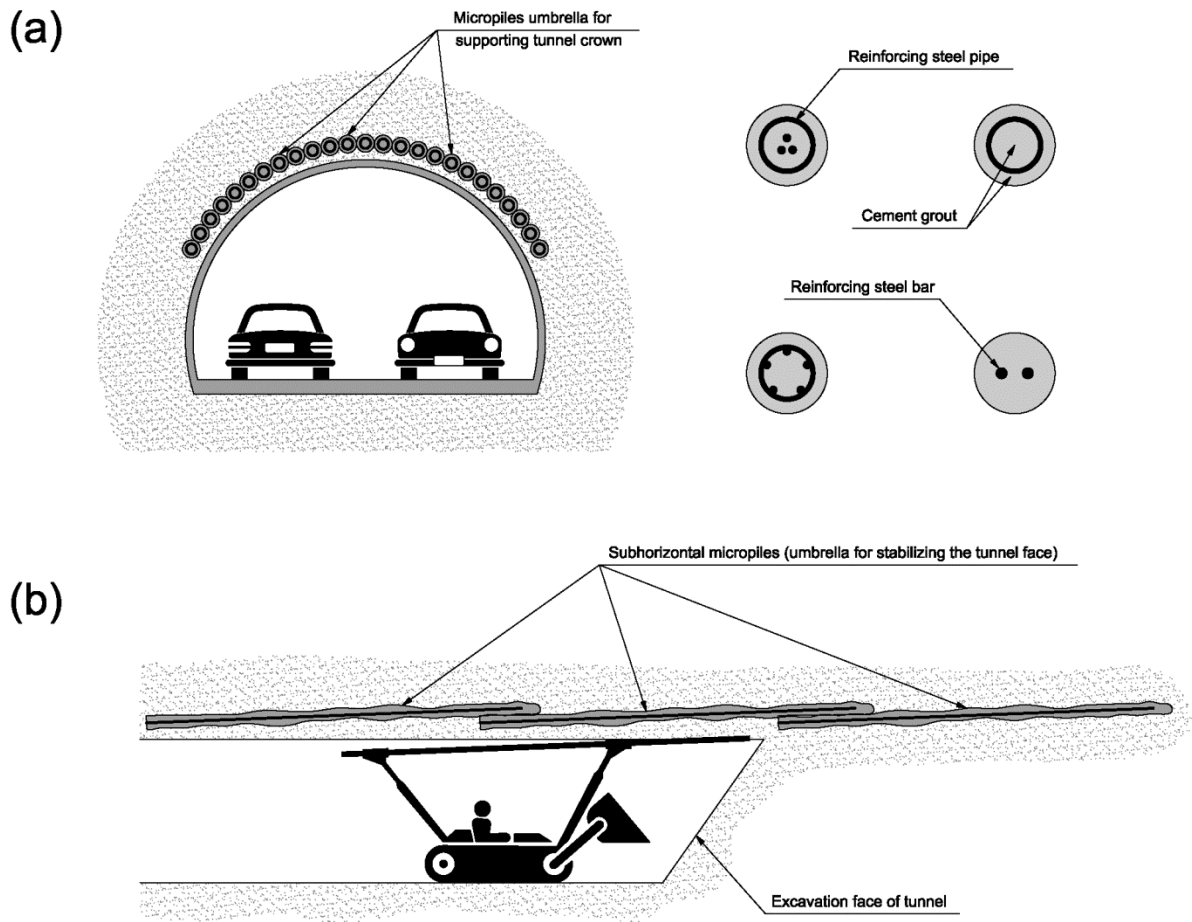


Fig. 1 – (a) Schematic representation of a road tunnel cross-section whose crown is supported by an umbrella of micropiles reinforced with steel pipe (left) and different sections of a micropile, depending on the type of reinforcement employed (right). (b) Excavation process of a tunnel face stabilized using a subhorizontal micropiles umbrella [3-5].

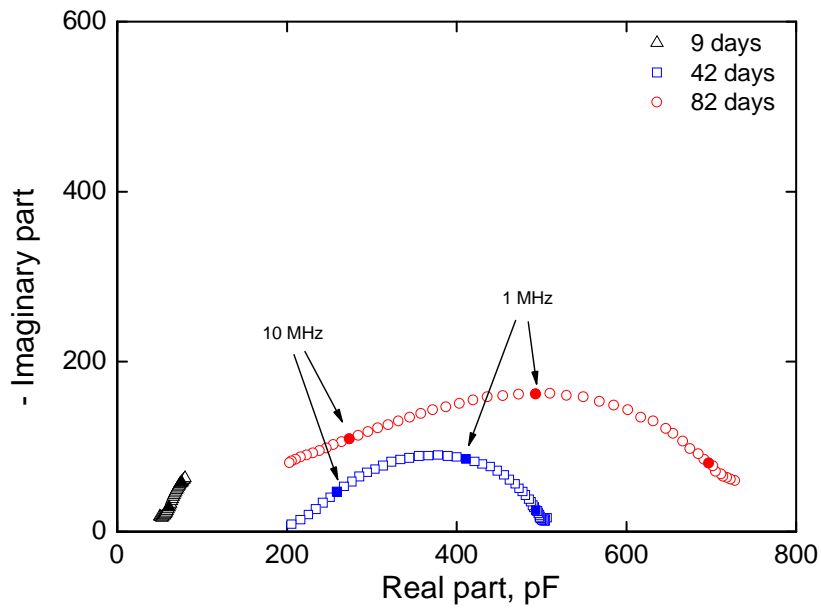


Fig. 2 –Evolution of the Cole–Cole plots for a CEM IV grout prepared with w:c ratio 0.4, obtained using the non-contacting method.

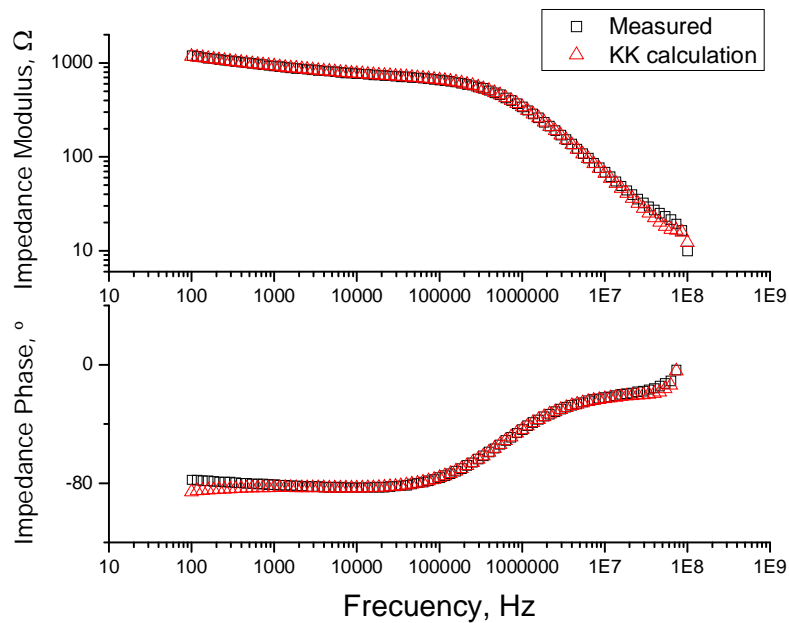


Fig. 3 –Example of an impedance spectrum obtained for a CEM IV grout with w:c ratio 0.5 at 54 hardening days, validated using the Kramers–Kronig (K–K) relations, see the text for details.

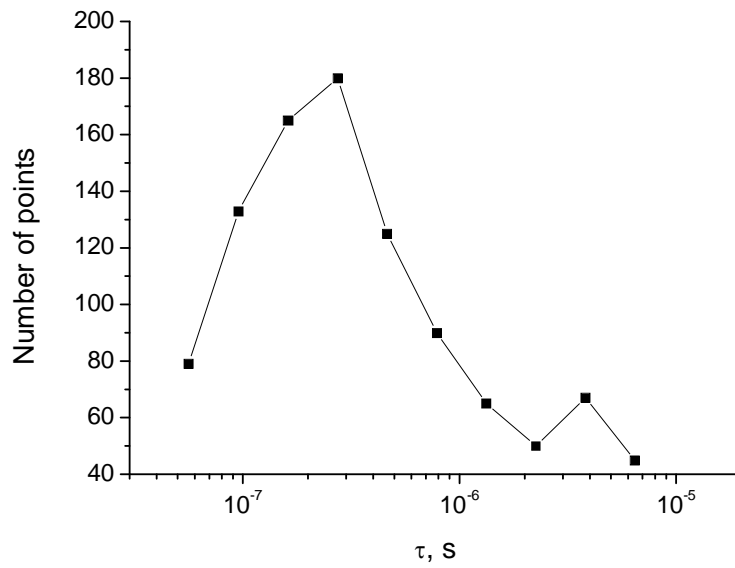


Fig. 4 –Differential impedance analysis of the impedance spectrum shown in Fig. 3. The presence of two maxima in the plot reveals the presence of two time constants in the impedance spectrum.

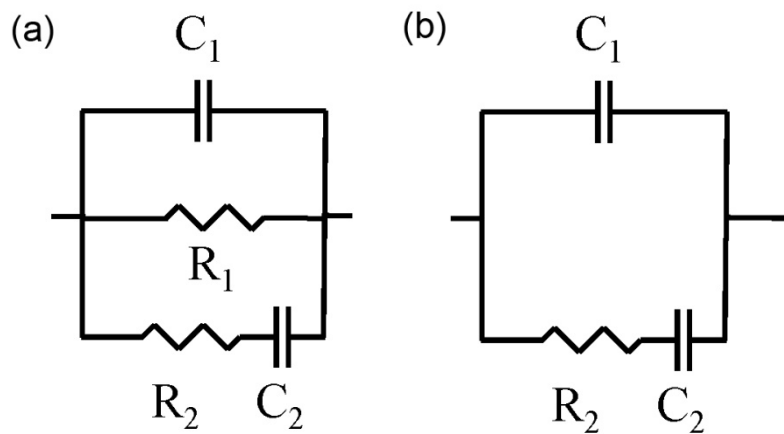


Fig. 5 – Equivalent circuits with two time constants proposed by Cabeza et al.[1] and used for the fitting of the impedance spectra obtained for samples using the contacting method (a) and the non-contacting method (b).

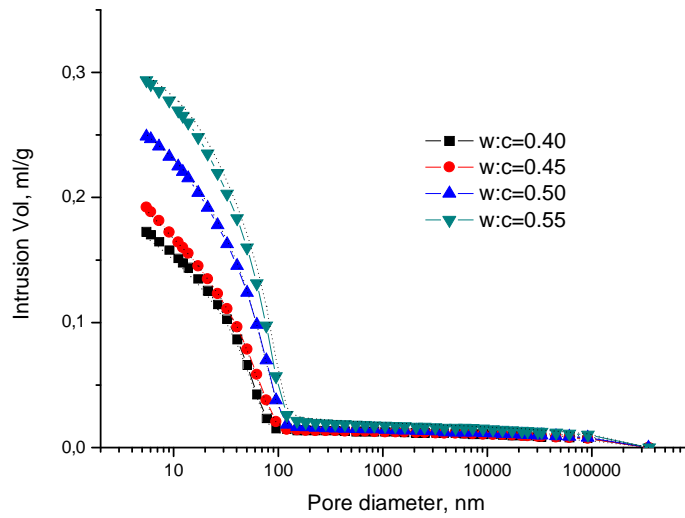


Fig. 6 Variation of the intrusion curves with w:c ratio for CEM I samples after 28 days hardening. Two samples were tested for each condition and the duplicate results are also shown in the graph

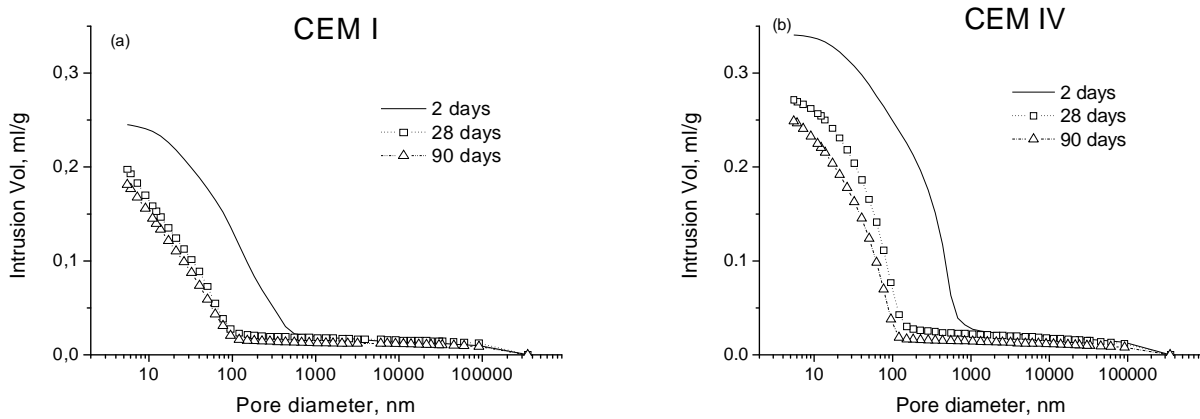


Fig. 7 Curves of intrusion volume for CEM I and CEM IV grouts with w:c ratio 0.5 for all the tested ages

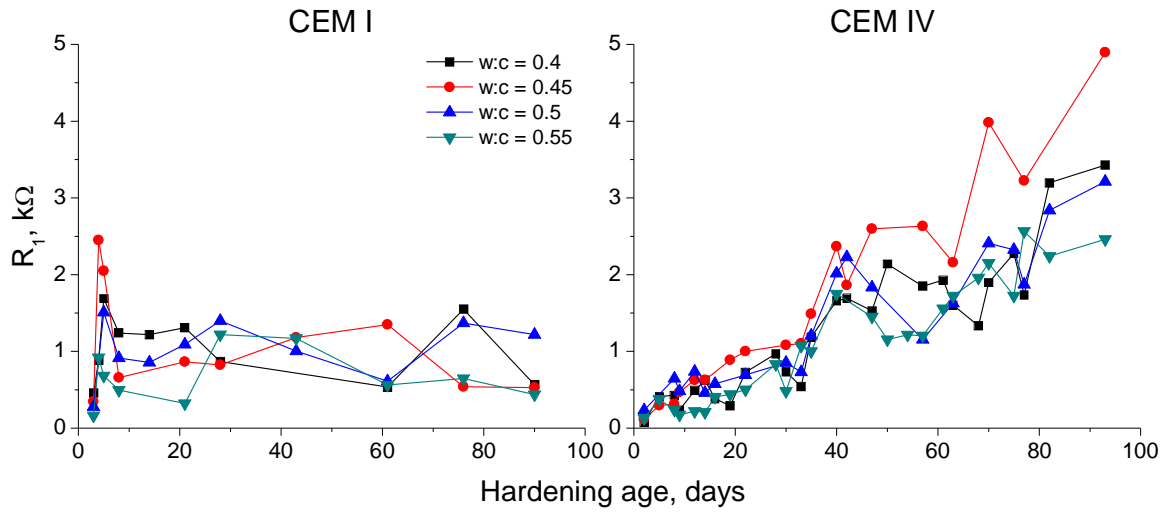


Fig. 8 –Results of resistance R_1 for CEM I and CEM IV grouts.

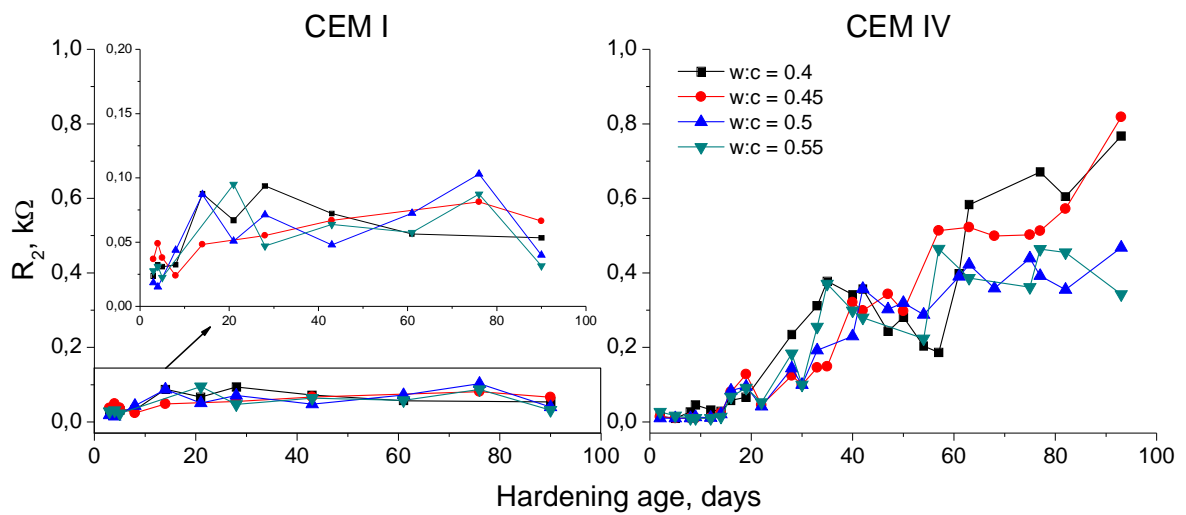


Fig. 9 –Results of resistance R_2 for CEM I and CEM IV grouts.

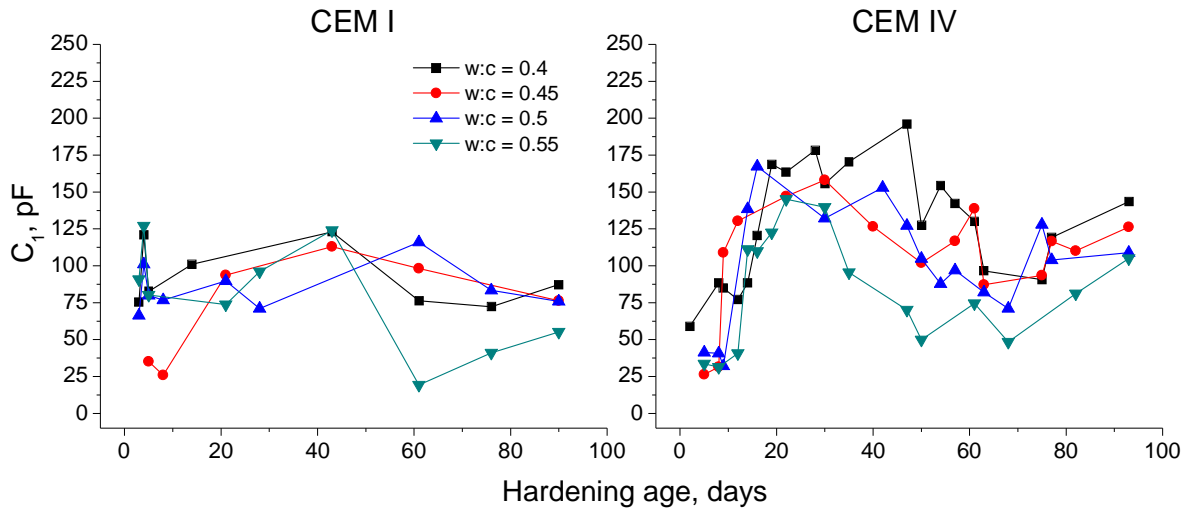


Fig. 10–Results of capacitance C_1 for CEM I and CEM IV grouts.

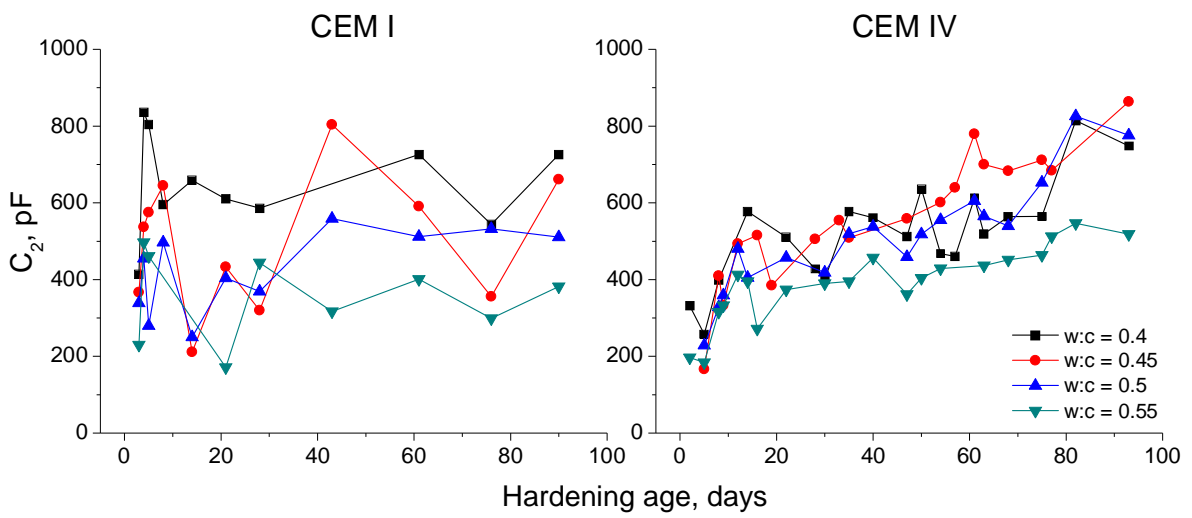


Fig. 11–Results of capacitance C_2 for CEM I and CEM IV grouts.

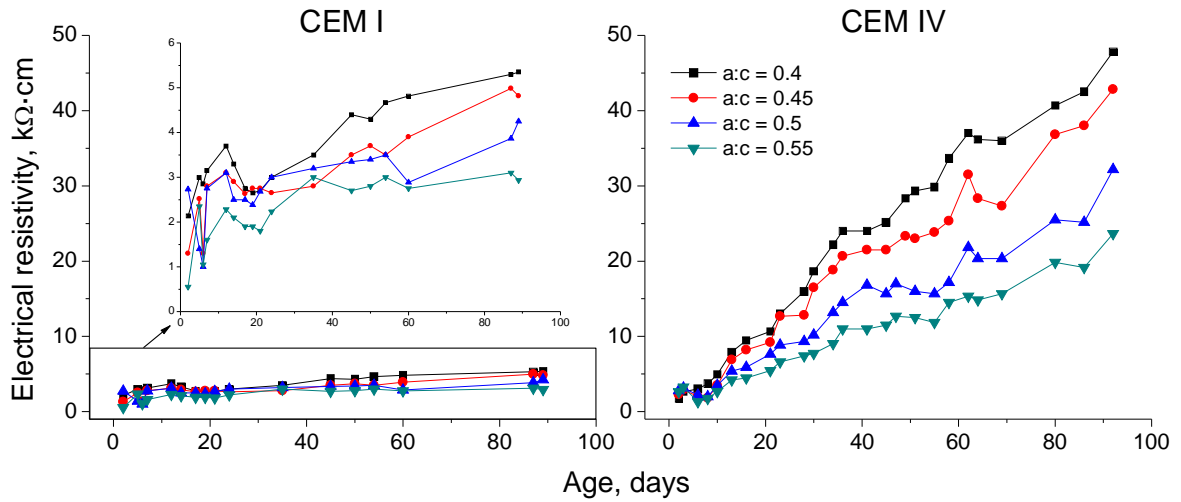


Fig. 12.- Results of electrical resistivity as a function of cement type, w:c ratio and age

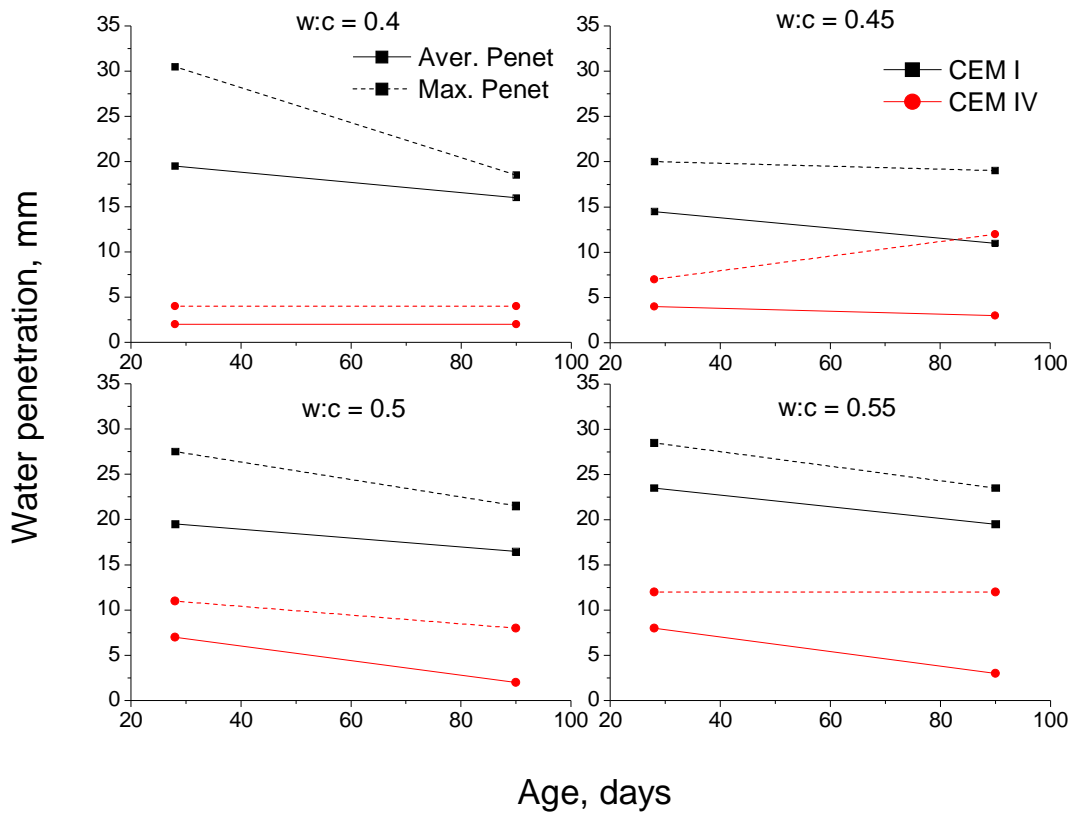


Fig. 13.- Results of water penetration under pressure as a function of cement type, w:c ratio and age. The average penetration is depicted using a continuous line, while the maximum penetration is depicted with a dotted line.

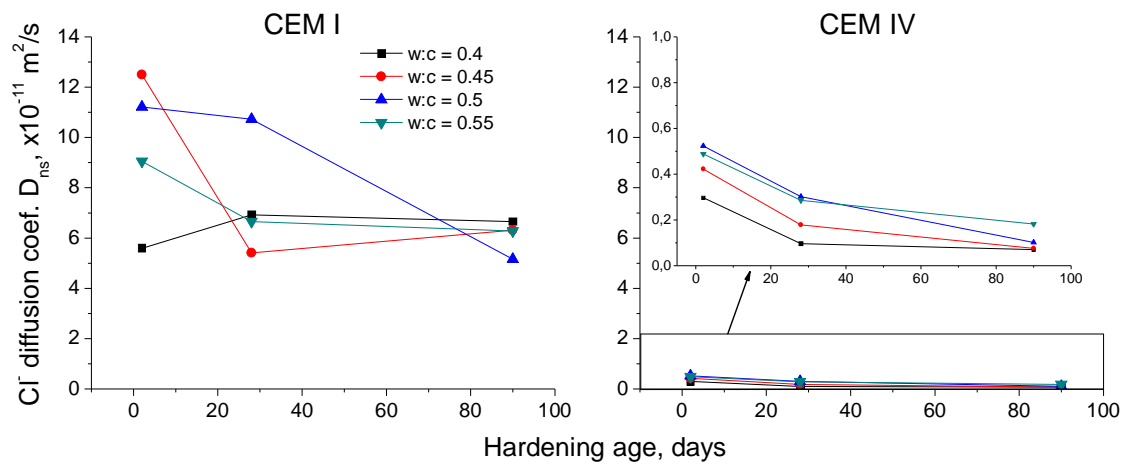


Fig. 14—Results of non-steady-state chloride diffusion coefficient (D_{ns}) for CEM I and CEM IV grouts.

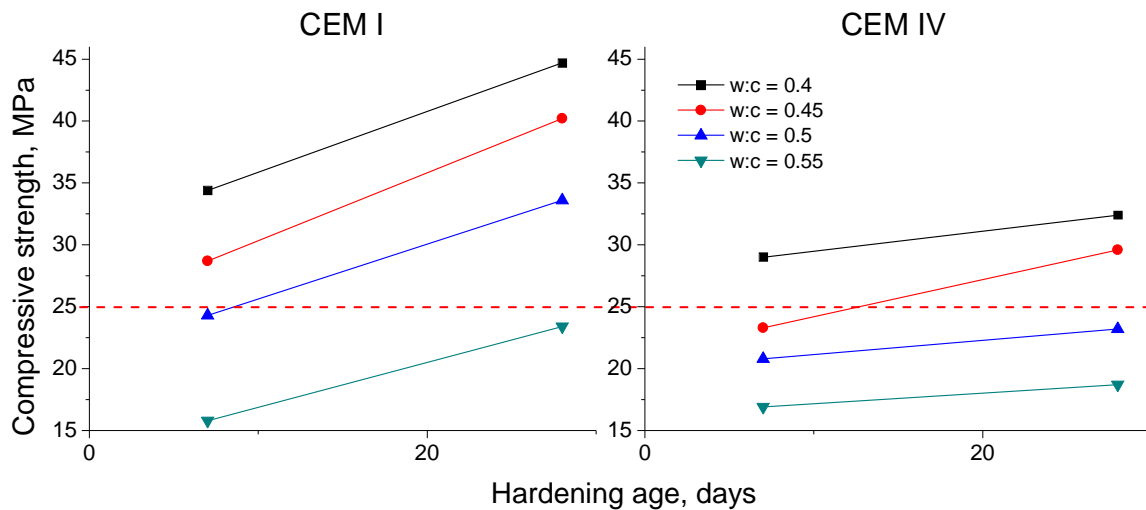


Fig. 15.- Results of compressive strength for CEM I and CEM IV grouts as a function of w:c ratio and age. Red line at 25 MPa denotes the minimum required strength at 28 days by the Spanish standard.

Table 1.- Results of fluidity of the samples made by letting flow the cement paste from the cone described in standard UNE-EN 1015-3

Cement type	CEM I				CEM IV			
w:c	0.4	0.45	0.5	0.55	0.4	0.45	0.5	0.55
Aver. diam., mm	13.75	16.65	21.25	24.15	16.35	20.4	22.9	24.4